Electron bulk heating in magnetic reconnection at Earth's magnetopause: Dependence on the inflow Alfvén speed and magnetic shear

T. D. Phan,[1] M. A. Shay,[2] J. T. Gosling,[3] M. Fujimoto,[4] J. F. Drake,[5] G. Paschmann,[6] M. Oieroset,[1] J. P. Eastwood,[7] and V. Angelopoulos[8]

Received 23 July 2013; revised 23 August 2013; accepted 28 August 2013; published 11 September 2013.

[1] We surveyed 79 magnetopause reconnection exhausts detected by the THEMIS spacecraft to investigate how the amount and anisotropy of electron bulk heating produced by reconnection depend on the inflow boundary conditions. We find that the amount of heating, ΔT_e, is correlated with the asymmetric Alfvén speed, $V_{AL,asym}$, based on the reconnecting magnetic field and the plasma density measured in both the high-density magnetosheath and low-density magnetospheric inflow regions. Best fit to the data produces the empirical relation $\Delta T_e = 0.017\ m_i V_{AL,asym}^2$, indicating that the amount of heating is proportional to the inflowing magnetic energy per proton-electron pair, with ~1.7% of the energy being converted into electron heating. This finding, generalized to symmetric reconnection, could account for the lack of electron heating in typical solar wind exhausts at 1 AU, as well as strong heating to keV energies common in magnetotail exhausts. We also find that the guide field suppresses perpendicular heating.
Citation: Phan, T. D., M. A. Shay, J. T. Gosling, M. Fujimoto, J. F. Drake, G. Paschmann, M. Oieroset, J. P. Eastwood, and V. Angelopoulos (2013), Electron bulk heating in magnetic reconnection at Earth's magnetopause: Dependence on the inflow Alfvén speed and magnetic shear, *Geophys. Res. Lett.*, *40*, 4475–4480, doi:10.1002/grl.50917.

1. Introduction

[2] Magnetic reconnection is a universal plasma process that converts magnetic energy into plasma jetting and thermal and suprathermal plasma heating. While plasma jetting is well established, both theoretically and observationally, the mechanisms whereby plasma (especially electron) heating occur in collisionless plasma is still poorly understood. The large majority of observational and theoretical studies to date have been focused on suprathermal electron energization, not on bulk heating. While suprathermal electrons are important in their own right, a more basic unresolved problem is the reconnection-associated bulk heating of electrons, i.e., the heating of the thermal population, which contains most of the electrons.

[3] In situ observations in the magnetosphere, solar wind, and magnetosheath have produced conflicting findings regarding the presence or absence of electron heating in reconnection exhausts, as well as the anisotropy of heating. Substantial electron bulk heating (in the 600 eV to 2 keV range) is typically observed in reconnection exhausts in the magnetotail (J. Liu, private communication, 2013). Electron bulk heating of tens of eV (i.e., two orders of magnitude lower than tail heating) has also been reported at the magnetopause [e.g., *Gosling et al*., 1986] and recently in a magnetosheath reconnection exhaust [*Phan et al*., 2011]. Contrary to these reports and the expectation that reconnection always results in bulk electron heating, *Gosling et al*. [2007] reported neither thermal electron heating nor suprathermal electron energization in several solar wind reconnection exhausts they identified.

[4] There are also differences in the reported anisotropy of electron bulk heating. Heating observed in near-Earth magnetotail exhausts tends to be roughly isotropic [e.g., *Chen et al*., 2008], while a magnetosheath exhaust reported by *Phan et al*. [2011] showed only parallel heating. These striking differences in the electron heating properties in different regions in space suggest that the degree and anisotropy of electron heating depend strongly on plasma parameter regimes and/or boundary conditions.

[5] In this paper, we report the results of a statistical study of electron bulk heating at the magnetopause based on 79 reconnection exhausts detected by the THEMIS spacecraft. We find that the degree of heating depends on the inflow Alfvén speed, while the heating anisotropy depends on the guide field/magnetic shear.

2. THEMIS Data Sets

[6] The data set consists of previously reported dayside low-latitude reconnection exhausts detected by THEMIS D in 2008 [*Phan et al*., 2013], as well as exhausts from THEMIS E in 2009. The reconnection exhausts were identified based on the presence of accelerated magnetosheath plasma flows across the magnetosheath edge of the magnetopause, with correlated or anticorrelated changes in the velocity and magnetic field vectors. In events that showed the presence of accelerated flows but where the agreement with the predicted flows from the Walen relation [e.g., *Paschmann et al*., 1986] was less than 50%, we further required the presence of interpenetrating magnetosheath and cold magnetospheric ions to ensure magnetic connection across the magnetopause. In order to investigate the electron temperature change across the magnetopause, we required

[1]University of California, Berkeley, California, USA.
[2]University of Delaware, Newark, Delaware, USA.
[3]University of Colorado Boulder, Boulder, Colorado, USA.
[4]ISAS, Kanagawa, Japan.
[5]University of Maryland, College Park, Maryland, USA.
[6]MPE, Garching, Germany.
[7]Imperial College London, London, UK.
[8]University of California, Los Angeles, California, USA.

Corresponding author: T. D. Phan, University of California, 7 Gauss Way, Berkeley, CA 94720, USA. (phan@ssl.berkeley.edu)

0094-8276/13/10.1002/grl.50917

that the inflow magnetosheath electron temperature be stable and free of leaked high-energy magnetospheric electrons. With these restrictions, 32 THEMIS D and 47 THEMIS E exhausts were found to be appropriate for this study.

[7] The ion and electron temperatures used in the present study are moments of the distributions. As will be shown below, the electron temperature moment is generally representative of the core (Maxwellian) part of the distribution.

3. Magnetopause Reconnection Exhausts With and Without Substantial Electron Heating

[8] In this section, we describe two magnetopause exhausts to illustrate the varying amount of electron heating in magnetopause reconnection as well as our methodology in the statistical survey to evaluate the amount of bulk heating of magnetosheath electrons entering into the exhaust and to determine the inflow boundary conditions.

3.1. A Reconnection Exhaust With Substantial Electron Bulk Heating

[9] The left panels of Figure 1 show an outbound magnetopause crossing by THEMIS D at low latitude near the subsolar point (11.9 MLT). We describe the event backward in time, going from the magnetosheath to the magnetosphere as we investigate the heating of the entering magnetosheath electrons. A plasma jet directed in the –L direction and having a flow speed of ~400 km/s relative to that in the magnetosheath (Figure 1b) was embedded in the magnetopause current layer (15:12–15:14:30 UT, between the leftmost red vertical dotted line and the rightmost black dashed line). The magnetic shear across the magnetopause was ~173° (Figure 1a).

[10] Across the magnetosheath edge of the magnetopause, both parallel and perpendicular electron temperatures increased abruptly, from ~50 eV (in the magnetosheath) to ~120 eV, and increased even further deeper within the exhaust. The heating of the entering magnetosheath electrons is also evident in the electron energy-time spectrogram (Figure 1e), which shows an upward energy shift at the magnetosheath edge of the magnetopause. Figure 1i shows representative electron distributions in the magnetosheath (black curve) and in the reconnection exhaust (red curve); the overlaid Maxwellian dashed curves correspond to the density and temperature moments of the entire electron distributions. The good fit between the Maxwellians and the low-energy electron spectra indicates that the temperature is dominated by the core electrons of magnetosheath origin, with suprathermal electrons (> 300 eV in the magnetosheath and > 1 keV in the exhaust) contributing little to the temperature moments.

[11] Figure 1f shows that the fluxes of 10 keV and 5 keV electrons (mostly of magnetospheric origin) decreased sharply at the magnetospheric edge of the magnetopause, at ~15:12:05 UT, while a small amount remained until ~15:13:10 UT. Thus, to study the amount of magnetosheath electron heating that occurred, we only consider the interval from the magnetosheath edge of the magnetopause to the location just before the magnetospheric electrons first appear (at 15:13:10 UT, marked by the green vertical line) to avoid contamination from magnetospheric electrons. The location where magnetospheric electrons first appear also marks the location where the magnetosheath density drops significantly. The average and standard deviation of the exhaust electron temperature in this exhaust interval were $\sim 115 \pm 14$ eV; thus, the average amount of electron heating for this event was $\Delta T_e \sim 70 \pm 14$ eV. If we consider the parallel and perpendicular heating separately, the amount of parallel and perpendicular heating were $\Delta T_{e\|} = 87 \pm 11$ eV and $\Delta T_{e\perp} = 61 \pm 16$ eV, respectively.

[12] The magnetosheath boundary conditions were determined by averaging over a stable magnetosheath interval immediately adjacent to the magnetopause (between the two red vertical dotted lines). For this event, the magnetosheath ion and electron β based on the reconnecting magnetic field component were 0.44 and 0.051, respectively, and the ion Alfvén speed based on the reconnecting field was 414 km/s.

3.2. A Reconnection Exhaust With Essentially no Electron Bulk Heating

[13] The right panels of Figure 1 show an exhaust observed during an inbound magnetopause crossing by THEMIS D at low latitude near the subsolar point (11.5 MLT). The magnetic shear across the magnetopause was ~90° (Figure 1j). Embedded in the magnetopause current layer (15:44:43–15:45:20 UT, between the rightmost red vertical dotted line and the leftmost black dashed line) was a plasma jet flowing in the −L direction with a speed (relative to magnetosheath flow) close to 120 km/s (Figure 1k).

[14] In contrast to the previous event, the electron temperature did not increase at the magnetosheath edge of the exhaust and remained roughly constant until 15:45:12 UT when hot (5–10 keV) magnetospheric electrons began to appear (Figure 1o). The lack of bulk heating of entering magnetosheath electrons is also evident in the electron spectrogram, which shows essentially no variations across the magnetopause and exhaust. Similarly, Figure 1r shows that the electron spectra in the magnetosheath (black curve) and in the reconnection exhaust (red curve) were nearly identical. ΔT_e for this exhaust was only 1.2 ± 0.7 eV and $\Delta T_{e\|}$ and $\Delta T_{e\perp}$ were only 0.6 ± 0.4 eV and 1.7 ± 1.3 eV, respectively.

[15] For this event, the magnetosheath ion and electron β_L based on the reconnecting magnetic field component (averaged over the interval between the two red dotted lines) were ~6.4 and ~1.65, respectively, and the ion Alfvén speed based on the reconnecting field was ~59 km/s.

[16] The key parameters responsible for the differences in bulk electron heating in the above-described events appear to be the magnetosheath electron β and Alfvén speed, and the current sheet shear angle. The purpose of the statistical survey below is to reveal which of these or other parameters control electron bulk heating and anisotropy in magnetopause reconnection exhausts.

4. Statistical Survey

4.1. Parameters Controlling the Degree of Electron Bulk Heating

[17] Using the set of 79 reconnection exhausts described in section 2, we examined how ΔT_e depends on plasma and field conditions on the opposite sides of the magnetopause. We found that ΔT_e does not depend on any purely magnetospheric parameters but does clearly depend on a number of magnetosheath parameters. The electron β based on the number density N_{sh}, electron temperature $T_{e,sh}$, and the reconnecting field component $B_{L,sh}$ measured n the magnetosheath adjacent to the magnetopause ($\beta_{eL,sh} = 2\mu_0 N_{sh} k T_{e,sh} / B_{L,sh}^2$) is one such parameter.

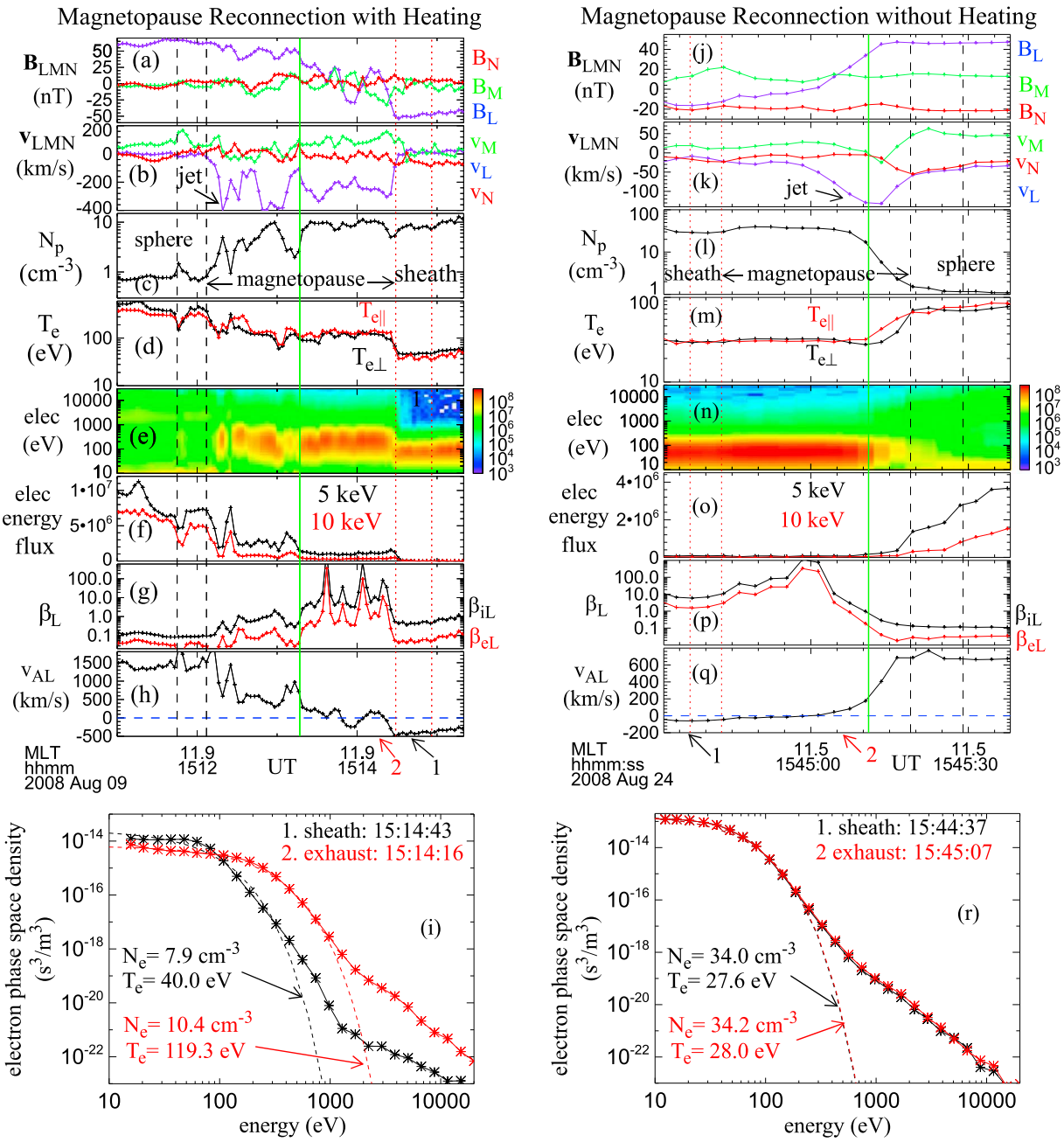

Figure 1. Examples of electron heating (left panels) and no heating (right panels) in magnetopause reconnection. (a, j) the magnetic field in LMN minimum variance coordinates [*Sonnerup and Cahill*, 1967], (b, k) ion velocity in LMN, (c, l) ion number density, (d, m) parallel and perpendicular electron temperatures, (e, n) electron energy spectrogram in energy flux (eV s^{-1} cm^{-2} $ster^{-1}$ eV^{-1}), (f, o) energy flux of 5 keV and 10 keV electrons, (g, p) ion and electron β based on the reconnecting field component B_L, (h, q) Alfvén velocity based on B_L, (i, r) electron spectra in the magnetosheath (black) and in the exhaust (red), with overlaid Maxwellian distributions using measured density and temperature moments. Labels "1" and "2" under Figures 1h and 1q point to the times of the cuts shown in Figures 1i and 1r. The (dotted) red and (dashed) black pairs of vertical lines denote the magnetosheath and magnetospheric intervals that define the boundary conditions of the magnetopause current sheet. The green vertical line denotes the innermost location of the exhaust for the computation of the average exhaust electron temperature.

Figure 2a shows that ΔT_e tended to decrease with increasing $\beta_{eL,sh}$. We also examined the dependence of ΔT_e on each of the separate parameters contributing to $\beta_{eL,sh}$. ΔT_e tended to increase with increasing $B_{L,sh}$ (Figure 2b) and tended to decrease with increasing N_{sh} (Figure 2c). However, there was no systematic dependence on $T_{e,sh}$ (Figure 2d).

[18] Since ΔT_e depends on the magnetosheath reconnecting field and density but not on the magnetosheath electron temperature, the genuine controlling parameter is likely to be the Alfvén speed, not β. Figure 2e shows that the electron bulk heating is indeed well correlated with the Alfvén speed based on the reconnecting field in the magnetosheath, $V_{AL,sh}$. In fact,

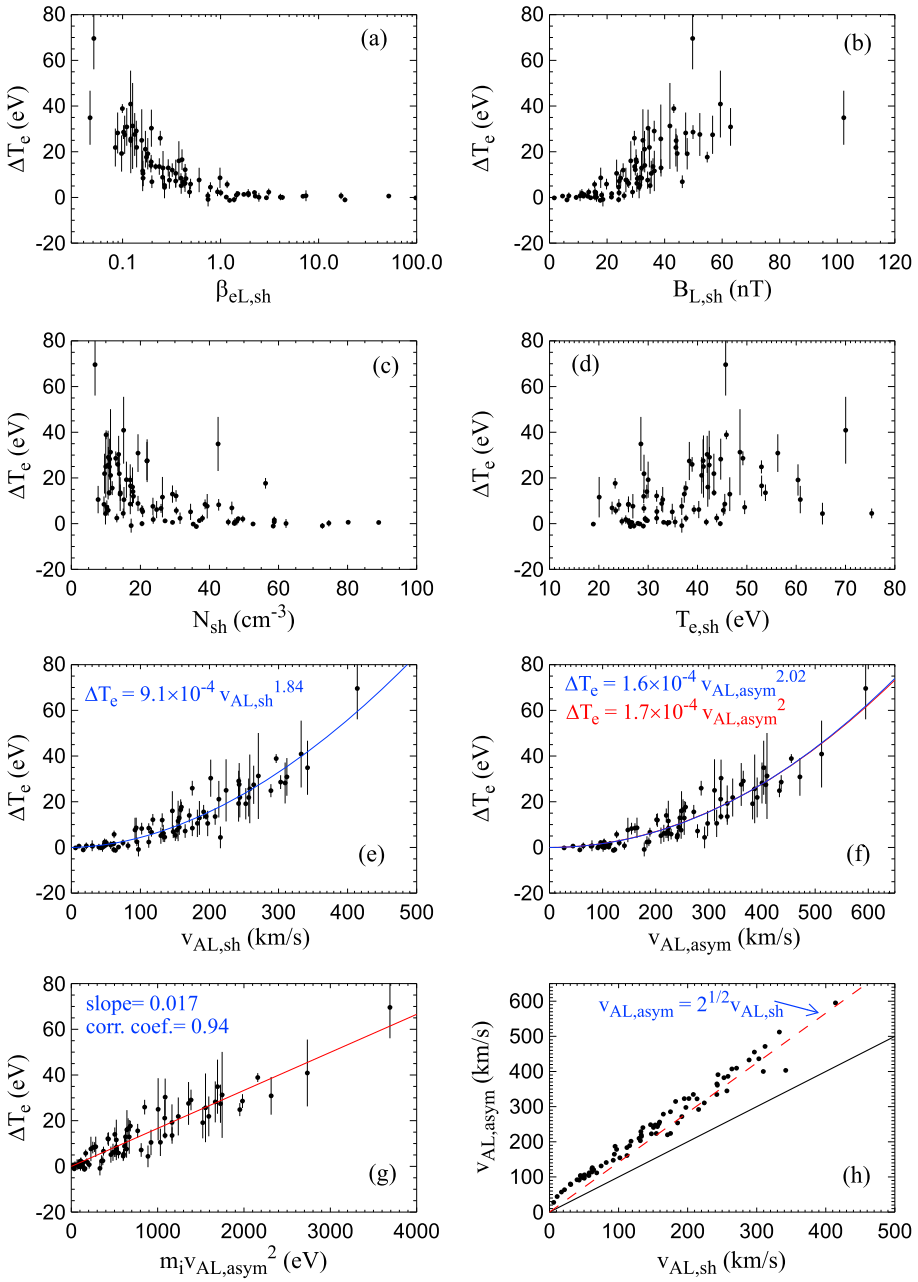

Figure 2. Electron heating as a function of (a) magnetosheath electron β based on the reconnecting field component, (b) magnetosheath reconnecting field component, (c) magnetosheath proton number density, (d) magnetosheath electron temperature, (e) magnetosheath Alfvén speed based on the reconnecting field component, (f) hybrid asymmetric inflow Alfvén speed, and (g) total inflowing magnetic energy. (h) The magnetosheath Alfvén speed versus the asymmetric Alfvén speed.

the dependence on $V_{AL,sh}$ is clearer (less data scatter) than on the reconnecting field and plasma density individually. The dependence on $V_{AL,sh}$, however, is not linear. To deduce the power of the $V_{AL,sheath}$ dependence, we fit the data to the function $\Delta T_e = \text{constant}*V_{AL,sh}^{power}$. The best fit gives a power of 1.84, which is close to 2.

[19] Figure 2f shows, however, that ΔT_e correlates equally well with the combined inflow Alfvén speed in asymmetric reconnection, $V_{AL,asym} = [B_{L,sh}B_{L,sph}(B_{L,sh}+B_{L,sph})/\mu_0(\rho_{sh}B_{L,sph}+\rho_{sph}B_{L,sh})]^{0.5}$, where ρ is ion mass density and subscript "sph" denotes the magnetosphere [*Cassak and Shay*, 2007; *Swisdak and Drake*, 2007]. Fitting the data to the function $\Delta T_e = \text{constant}*V_{AL,asym}^{power}$ produces a power of 2.02 (blue curve in Figure 2f), which is essentially 2. Refitting the data to $V_{AL,asym}^2$ gives $\Delta T_e = 1.7\times10^{-4}\ V_{AL,asym}^2$ (red curve in Figure 2f), where ΔT_e and $V_{AL,asym}$ are in units of eV and km/s, respectively. The significance of the dependence on $V_{AL,asym}^2$ is that $m_i V_{AL,asym}^2$ represents the combined incoming magnetic energy per proton-electron pair from both sides of the current sheet, where m_i is the proton mass. The empirical relation can be reexpressed as $\Delta T_e = 0.017\ m_i V_{AL,asym}^2$ (Figure 2g). The linear relationship between ΔT_e and the inflow energy indicates that the amount of bulk electron heating is simply ~1.7% of the magnetic energy flowing into the exhaust. If we had used the peak electron temperature in the exhaust instead of the average exhaust temperature, the

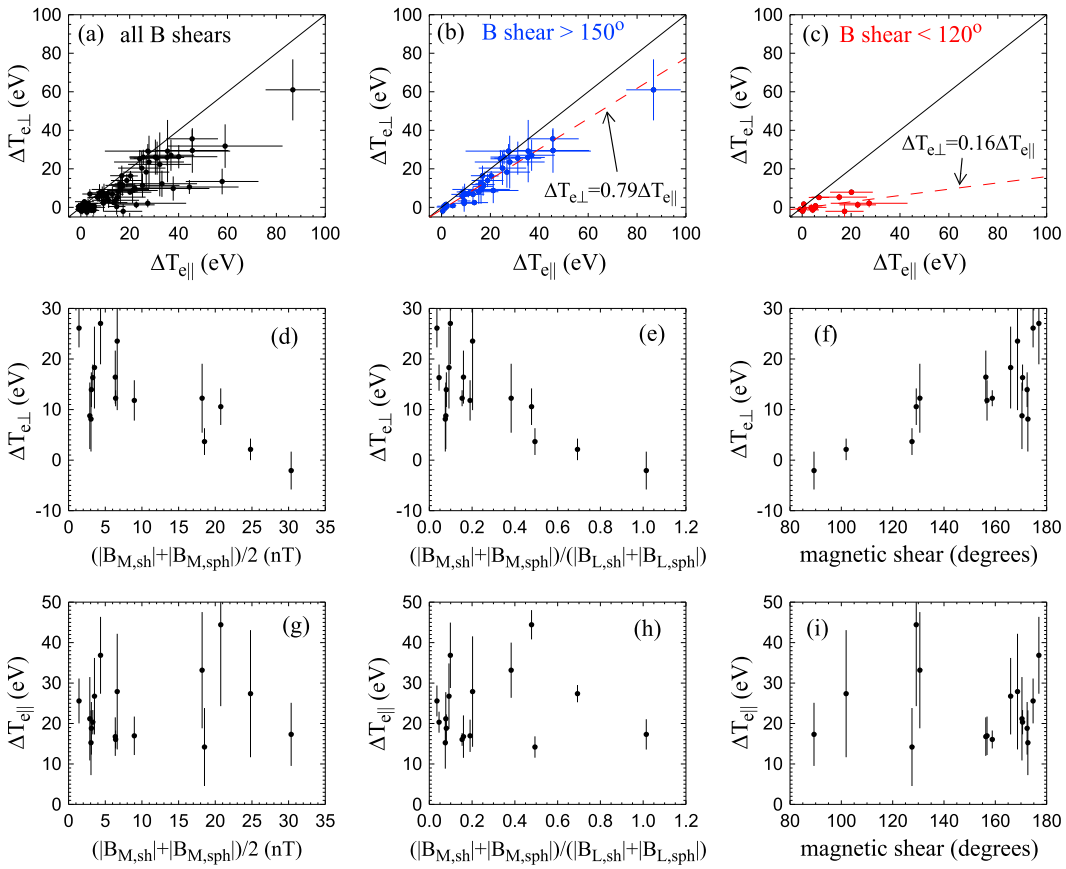

Figure 3. The anisotropy of electron heating and its guide field dependence. Perpendicular versus parallel heating for (a) all 79 events, (b) events with magnetic shear > 150°, and (c) events with magnetic shear < 120°. (d–f) Perpendicular heating versus the guide field, the guide field normalized to the reconnecting field, and the magnetic shear. (g–i) Parallel heating versus the guide field, the guide field normalized to the reconnecting field, and the magnetic shear. Figures 3d–3i are restricted to exhausts where 250 km/s < $|V_{AL,asym}|$ < 350 km/s.

empirical fraction would be ~2.3%. The small percentage indicates that the electrons are a minor recipient of the released energy in reconnection [see also *Eastwood et al.*, 2013].

[20] Finally, the relationship between $V_{AL,sh}$ and $V_{AL,asym}$ is shown in Figure 2h. For the present data set, the average magnetosheath to magnetospheric density ratio is large (~32). Thus, the incoming magnetic energy is distributed to about half the number of particles in the strongly asymmetric case as compared to the case of symmetric inflows. In this highly asymmetric density regime, $V_{AL,asym}$ reduces to ~$2^{1/2}V_{AL,sh}$ for approximately symmetric inflowing magnetic fields, which is the case for large $V_{AL,sh}$ events in Figure 2h.

4.2. Anisotropy of Electron Heating and the Guide Field Dependence

[21] In addition to examining the average electron heating, we have also investigated parallel and perpendicular electron heating separately. Figure 3a shows that parallel heating almost always exceeds perpendicular heating. Furthermore, the heating anisotropy depends on the magnetic shear across the magnetopause (i.e., the guide field). Figures 3b and 3c show that electron heating is more isotropic ($\Delta T_{e\perp}$ ~ 0.79$\Delta T_{e\parallel}$ on average) for large (>150°) magnetic shears than for low (<120°) magnetic shears ($\Delta T_{e\perp}$ ~ 0.16$\Delta T_{e\parallel}$ on average). There are a number of events with $\Delta T_{e\perp}$ < 0 (slight cooling), which tend to occur for low magnetic shears: $\Delta T_{e\perp}$<0 in 7 of 15 low magnetic shear (< 120°) cases (Figure 3c) but in only one of 38 high shear (>150°) cases (Figure 3b).

[22] Figures 3d–3f further illustrate the effect of the guide field on perpendicular heating. In order to separate the guide field effect from the dependence on the Alfvén speed, we restricted the data to 250 km/s < $|V_{AL,asym}|$ < 350 km/s (although the findings are qualitatively similar for other ranges of the Alfvén speed). Figures 3d and 3e show that there is a trend for a decrease in perpendicular heating with an increase in both the guide field and the guide field normalized to the reconnecting field. The perpendicular heating is almost completely suppressed when the normalized guide field reaches unity, at least in this Alfvén speed range. Equivalently, the amount of perpendicular heating decreases with decreasing magnetic shear (Figure 3f).

[23] In contrast to perpendicular heating, $\Delta T_{e\parallel}$ does not show any clear dependence on the guide field or the magnetic shear (Figures 3g–3i).

[24] Finally, the local magnetic shear measured at the THEMIS spacecraft may or may not be the same as the shear at the X-line because of the curved magnetopause. However, because the present data set is comprised of dayside low-latitude magnetopause crossings with magnetic shear > 45°, it is expected that the X-line would be close to the subsolar point and not far from the spacecraft. Furthermore, it is still

an open question whether the bulk of the electron heating occurs locally or in the vicinity of the X-line.

5. Summary and Discussions

[25] We have examined factors that appear to control the amount of electron bulk heating and its anisotropy. We found that the electron bulk heating is linearly proportional to the inflowing magnetic energy per proton-electron pair, $m_i V_{AL,asym}^2$. The empirical relation $\Delta T_e = 0.017\ m_i V_{AL,asym}^2$ indicates that ~1.7% of the magnetic energy is converted into electron bulk heating. Our finding should in principle be general and applicable to symmetric reconnection as well with $\Delta T_e = 0.017\ m_i V_{AL,inflow}^2$, or equivalently $0.017\ B_{L,inflow}^2/\mu_0 N_{inflow}$, where $V_{AL,inflow}$, $B_{L,inflow}$, and N_{inflow} are the inflow (upstream) Alfvén speed, reconnecting field, and density on both sides of the exhaust. The dependence of ΔT_e on $m_i V_{AL,inflow}^2$ is exactly equivalent to $\Delta T_e/T_{e,inflow} = 0.034/\beta_{eL,inflow}$, indicating that the percentage of electron heating relative to its initial temperature is substantial in low β plasmas. However, the dependence on $1/\beta_{eL,inflow}$ should be viewed with care; a set of events with all equal ΔT_e could have this dependence simply because both $\Delta T_e/T_{e,inflow}$ and $\beta_{eL,inflow}$ involve $T_{e,inflow}$.

[26] We also found that parallel heating almost always exceeds perpendicular heating and that the guide field suppresses perpendicular heating. This suggests that the heating is primarily field aligned, with subsequent perpendicular energy gain arising due to scattering or other processes, the effectiveness of which depends on the guide field.

[27] Although our finding of the linear dependence of electron heating on inflow energy suggests universality, our study pertains to highly asymmetric reconnection and covers a limited range of the inflow Alfvén speeds (27–595 km/s). Future studies should expand to higher Alfvén speeds as well as symmetric conditions to verify the universality of the present findings on the scaling with the inflow Alfvén speed as well as the percentage of inflow energy converted into electron bulk heating. Nevertheless, taken at their face value, these findings may be able to account for previous conflicting findings on the amount and anisotropy of electron heating observed in the various regions, as we now discuss.

[28] Our finding that electron heating becomes more isotropic as the guide field decreases is consistent with the near isotropic heating in magnetotail exhausts [*Chen et al*., 2008], which are generally associated with small (< 20%) guide field. It is also consistent with a reported magnetosheath event with the guide field roughly equal to the reconnecting field, which showed only parallel heating but no perpendicular heating [*Phan et al*., 2011].

[29] The empirical heating relation may provide an explanation for the reported lack of solar wind exhaust heating [*Gosling et al*., 2007]. At 1 AU, the Alfvén speed of the solar wind is typically ~ 50 km/s. For that value of V_{AL}, the predicted electron bulk heating based on our empirical formula is only ~0.45 eV, which is practically unmeasurable. However, our study suggests that stronger electron heating should occur in the solar wind closer to the Sun where the ambient solar wind Alfvén speed is higher, as well as in currents sheets at 1 AU with unusually large V_{AL}, such as those embedded in some interplanetary coronal mass ejections.

[30] Extrapolating our finding to the magnetotail plasma regime, where the typical Alfvén speed in the reconnection inflow (i.e., lobe) region is ~ 2000–3000 km/s (based on a typical density of 0.05 cm^{-3} [*Svenes et al*., 2008] and magnetic field of 20–30 nT), the expected electron heating would be in the 700 eV to 1.5 keV range, roughly consistent with the strong electron heating typically seen in magnetotail exhausts. Thus, although only 1.7% of the available magnetic energy goes into electron heating, for sufficiently high inflow Alfvén speeds, reconnection substantially increases the electron temperature.

[31] Similarly, higher Alfvén speeds in the magnetosheath plasma depletion layer (stronger field, lower density) associated with high-latitude magnetopause reconnection [*Fuselier et al*., 2000] should lead to much stronger electron heating compared to low-latitude reconnection.

[32] Finally, our empirical findings could potentially be used to evaluate the role of reconnection in bulk electron heating in solar and astrophysical contexts. For example, in the solar coronal region where the local Alfven speed is ~2200 km/s (based on B ~ 100 Gauss, N ~ $10^{10} cm^{-3}$), the electrons could be heated up to 10^7 K (or ~1 keV) by reconnection.

[33] **Acknowledgments.** We thank the THEMIS team for providing well-calibrated plasma and field data. This research was funded by NASA grants NNX08AO83G, NASS02099, NNX10AC01G, NNX08AO84G, NNX11AD69G, NNX13AD72G and NSF grants ATM-0645271 and AGS1202330.

[34] The Editor thanks Karlheinz Trattner and Hui Zhang for their assistance in evaluating this paper.

References

Cassak, P. A., and M. A. Shay (2007), Scaling of asymmetric magnetic reconnection: General theory and collisional simulations, *Phys. Plasmas*, *14*, 102114, doi:10.1063/1.2795630.

Chen, L. J., et al. (2008), Evidence of an extended electron current sheet and its neighboring magnetic island during magnetotail reconnection, *J. Geophys. Res.*, *113*, A12213, doi:10.1029/2008JA013385.

Eastwood, J. P., T. D. Phan, J. F. Drake,M. A. Shay, A. L. Borg, B. Lavraud, and M. G. Taylor (2013), Energy partition in magnetic reconnection in Earth's magnetotail, *Phys. Res. Lett.*, *110*(22), 225001.

Fuselier, S. A., S. M. Petrinec, and K. J. Trattner (2000), Stability of the high-latitude reconnection site for steady northward IMF, *Geophys.Res. Lett.*, *27*, 473–476.

Gosling, J. T., M. F. Thomsen, S. J. Bame, and C. T. Russell (1986), Accelerated plasma flows at the near-tail magnetopause, *J. Geophys. Res.*, *91*, 3029–3041.

Gosling, J. T., S. Eriksson, T. D. Phan, D. E. Larson, R. M. Skoug, and D. J. McComas (2007), Direct evidence for prolonged magnetic reconnection at a continuous X-line within the heliospheric current sheet, *Geophys. Res. Lett.*, *34*, L06102, doi:10.1029/2006GL029033.

Paschmann, G., I. Papamastorakis, W. Baumjohann, N. Sckopke, C. W. Carlson, B. U. Sonnerup, and H. Lühr (1986), The magnetopause for large magnetic shear: AMPTE/IRM observations, *J. Geophys. Res.*, *91*, 11,099–11,115, doi:10.1029/JA091iA10p11099.

Phan, T. D., T. E. Love, J. T. Gosling, G. Paschmann, J. P. Eastwood, M. Oieroset, V. Angelopoulos, J. P. McFadden, D. Larson, and U. Auster (2011), Triggering of magnetic reconnection in a magnetosheath current sheet due to compression against the magnetopause, *Geophys. Res. Lett.*, *38*, L17101, doi:10.1029/2011GL048586.

Phan, T. D., G. Paschmann, J. T. Gosling, M. Oieroset, M. Fujimoto, J. F. Drake, and V. Angelopoulos (2013), The dependence of magnetic reconnection on plasma β and magnetic shear: Evidence from magnetopause observations, *Geophys. Res. Lett.*, *40*, 11–16, doi:10.1029/2012GL054528.

Sonnerup, B. U. O., and L. J. Cahill (1967), Magnetopause structure and attitude from Explorer 12 observations, *J. Geophys. Res.*, *72*, 171.

Svenes, K. R., B. Lybekk, A. Pedersen, and S. Haaland (2008), Cluster observations of near-Earth magnetospheric lobe plasma densities – A statistical study, *Ann. Geophys.*, *26*, 2845–2852, doi:10.5194/angeo-26-2845-2008.

Swisdak, M., and J. F. Drake (2007), Orientation of the reconnection X-line, *Geophys. Res. Lett.*, *34*, L11106, doi:10.1029/2007GL029815.